HRTEM Reconstruction of A-polar NWs

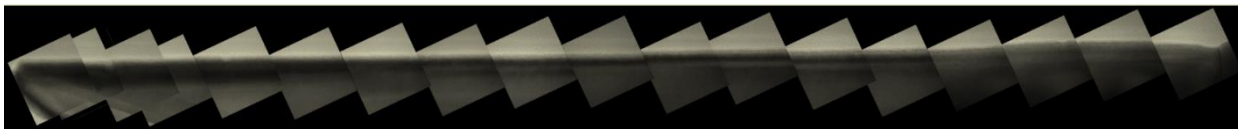

Figure SI1: HRTEM reconstruction of the wire shown in figure F1(a), demonstrating the defect-free nature of wire for areas far from the root.

Discussion on the Morphology of A-polar NWs

To understand the tapering of the A-polar wires, low magnification HAADF-STEM images are used. In this imaging mode, the intensity is proportional to $z^{\alpha}h$, in which z and h are the atomic number and the thickness of the specimen [1] and $1 < \alpha < 2$. When probing GaAs NWs, one can use the variation of the HAADF intensity to probe the thickness variation of the cross section of the NWs. Figure SI2(a) shows one such HAADF image. Figure SI2 (b) shows a schematic view of the hexagonal cross section of the nanowire, while figure SI2(c) demonstrates the scan profile corresponding to point P9.

In order to characterize the cross section, we define these geometrical parameters:

$$l = AD, l' = BC = EF,\ h = BF = CE$$

The aspect ratio is defined as:

$$a = \frac{l - l'}{l'} = \frac{l}{l'} - 1$$

For a perfectly regular hexagon, this aspect ratio will be equal to one. We notice that for $l = l'$, the aspect ratio will be zero and the cross section will have a rectangular shape. Aspect ratios less than one show elongation along AD direction, as shown in Figure SI2(b).

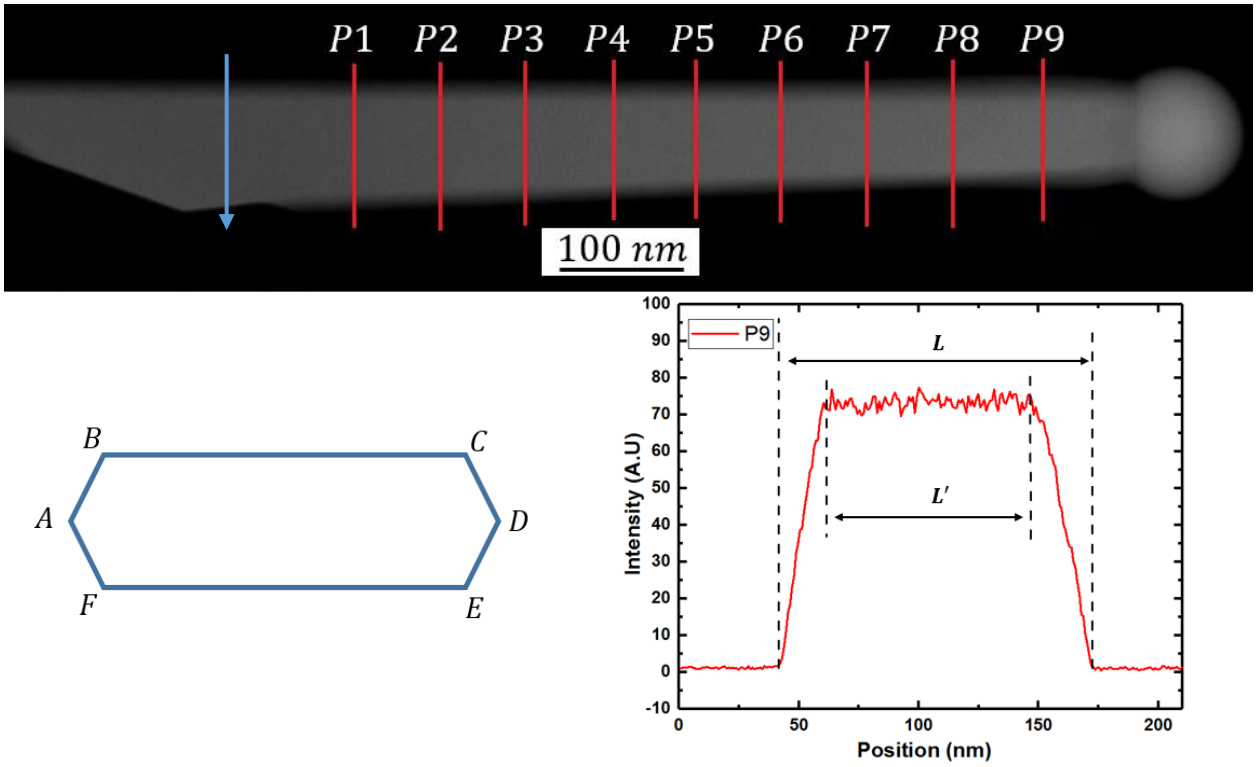

Figure SI2. (a) low magnification HAADF image of an A-polar wire used to extract the geometrical parameters of the cross section. (b) schematic view of the cross section of an A-polar wire.(c) profile scan corresponding to P9, demonstrating the determination of the parameters l and l'.The scan is done in the direction of the blue arrow in Figure S1(a).

Figure SI3 summarizes the variation of the geometrical parameters of the cross section for points P1 to P9 as shown. This graph indicates that areas close to the root of the root of the NW, the aspect ratio is less than one and the hexagonal cross section is stretched along the along its AD diagonal. This cross section entails that the Ga droplet that drives the growth is ellipsoidal rather than spherical. It is well known that the droplets in contact with solid prefer to adopt spherical shapes, as spherical shape minimizes the total surface for a given volume, hence minimizing the total surface energy. As the nanowire growth continues, the droplet gradually tries to morph into spherical shape, and this causes the cross section of the nanowire to approach a regular hexagon shape. This process happens by reduction in both l and l', which is in turn responsible for the tapered shape of the nanowire. We notice that for point P9, the aspect ratio is very close to one and the cross section is close to a regular hexagon. The thickness of the hexagonal cross section for this point is then calculated assuming a perfectly regular hexagon with geometrical parameters l and l'. The cross section thickness for other points is then calculated using the relative intensity of HAADF scans for those points compared to point P9. We observe that the reduction in l and l' is accompanied by an increase in the thickness. This indicates the NWs have low thicknesses in the areas close to the root.

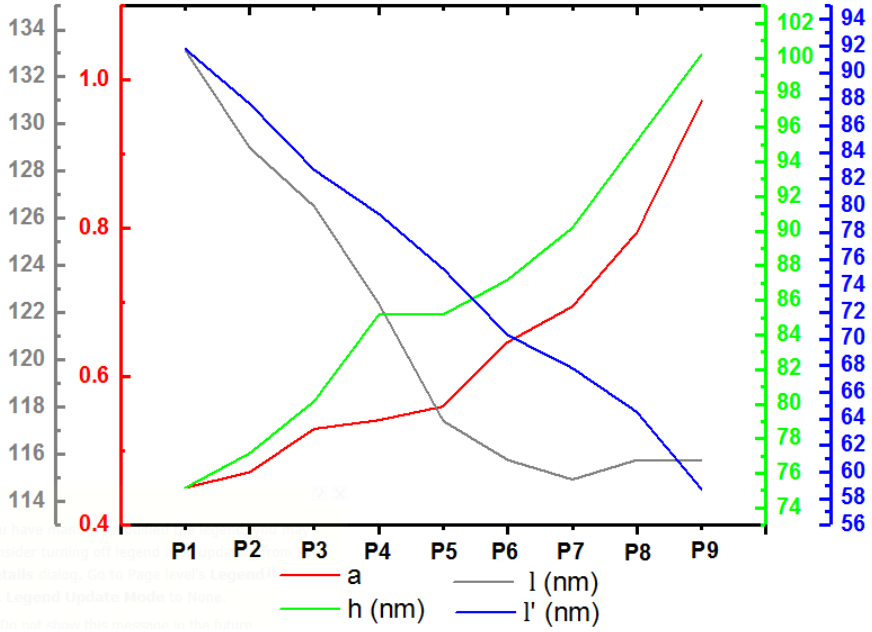

Figure SI3. Decrease in values of l and l' and increase in thickness and aspect ratio of the nanowire growth progresses from point P1 to P9. Reduction in l is responsible for the tapered shape of the NW, while the increase in the aspect ratio and the thickness of the wire indicate that the cross section approaches a regular hexagon shape as growth is progressed.

SEM images of samples discussed in the manuscript:

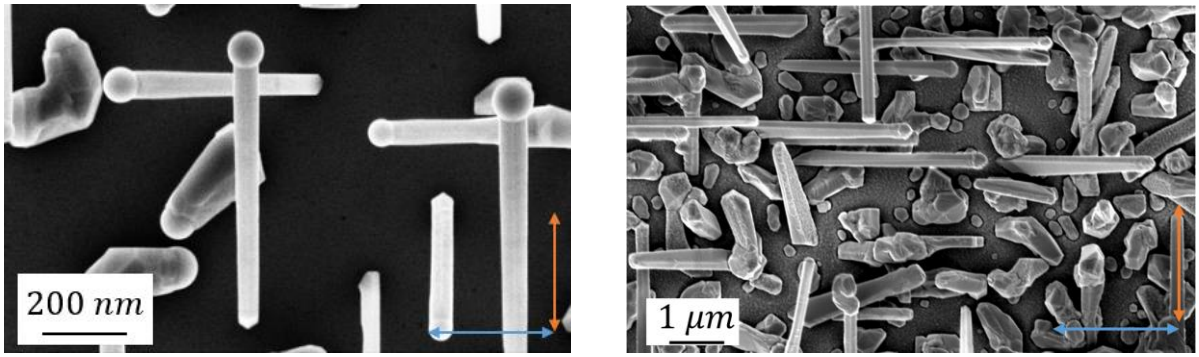

(a) (b)

Figure SI4. (a) and (b):Top view SEM image of sample discussed in Figure 5 and the core-shell sample discussed in Figure 6, respectively. The blue arrow shows the [111]A direction, while the orange arrow depict the [111]B.

Discussion on the insufficiency of ex-situ contact angle measurements

To reconcile the contradiction between our observations and the previously reported data, we refer to Figure 5(a) and 5(b) that depict the droplet configuration for A and B-polar NWs. We observe that the A-polar NWs are marked by a sudden shrinking in their diameter just below the droplet. This consistent characteristic of A-polar wires is absent in B-polar NWs. Figure SI4(a) and SI4(b) schematically demonstrate this behaviour. In this figure, the contact angles of A and B-polar NWs are depicted by α_A and α_B, respectively, while β_A shows the angle that the truncated growth front makes with the droplet. We note that, $\beta_A \cong \beta_A$ and $\alpha_A < \beta_B$. This implies that that, the truncated facet has higher surface energy than the B-polar surface.

The reduction in the diameters inadvertently imposes a sudden shrinking of the Ga droplet in A-polar NWs and this means that the contact angles measured by the ex-situ measurements might not be the same as the contact angles during the growth. As already mentioned, it has been previously discussed in the literature that central nucleation and formation of ZB phase happen at higher contact angles compared to TLP nucleation and WZ formation. However, the fact the last grown monolayers in A and B-polar wires show different nucleation mechanism and phases while having similar contact angle implies that the contact angle might not be sufficient to discriminate different growth mechanism in all the cases. Central nucleation and presence of truncated facets are believed to be necessary for formation of ZB [2,3]. As previously discussed, ZB phase is more favoured in low V/III ratios. This entails that increasing the V/III ratio at the last stage of growth makes the truncated growth front to become unfavourable. The shrinking of the diameter in A-polar NWs is caused by the fact that, at end stages of growth, the V/III ratio increases and the truncated facets start to disappear. This makes us believe that the truncated facets are bigger during the growth compared to what is observable in ex-situ setting. Since the B-polar wires are terminated by WZ phase, their growth front does not have any truncated facet and increased V/III does not change the geometry of their growth front. The absence of the shrinking behaviour in B-polar is a consequence of this fact. All in all, based on the discussions presented here, we conclude that a reasonable comparison of the contact angles in self-catalyzed GaAs NW growth is possible only by in-situ techniques. Even if not cooled down under As flux, different desorption rates of Ga and As atoms from the walls of the growth chamber and the sample will impose a change in the effective V/III ratio and cause a possible shift in the contact angle.

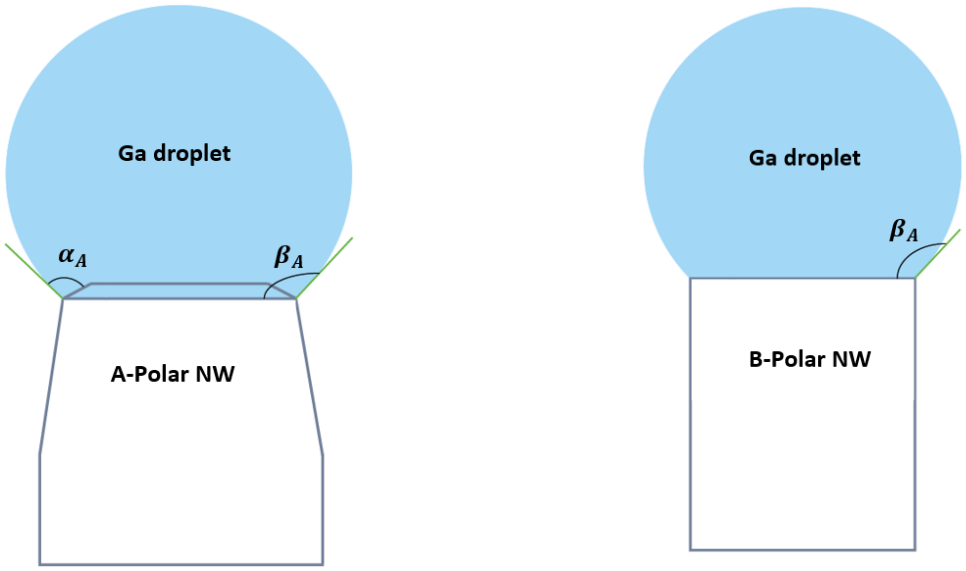

Figure SI(5): schematic view of the droplet configuration as observed by ex-situ setup for A and B-polar NWs.

1 C. B. Carter and D. B. Williams, Eds., *Transmission Electron Microscopy*, Springer International Publishing, Cham, 2016.

2 D. Jacobsson, F. Panciera, J. Tersoff, M. C. Reuter, S. Lehmann, S. Hofmann, K. A. Dick and F. M. Ross, *Nature*, 2016, **531**, 317–322.

3 C.-Y. Wen, J. Tersoff, K. Hillerich, M. C. Reuter, J. H. Park, S. Kodambaka, E. A. Stach and F. M. Ross, *Phys. Rev. Lett.*, 2011, **107**, 025503.